

## MUSCOVITE-BEARING GRANITES IN THE AFM LIQUIDUS PROJECTION

RICHARD N. ABBOTT, JR.

Department of Geology, Appalachian State University, Boone, North Carolina 28608, U.S.A.

### ABSTRACT

The AFM projection ( $A = Al_2O_3 - K_2O - Na_2O - CaO$ ,  $F = FeO$ ,  $M = MgO$ ) provides a convenient way to illustrate the liquidus reactions involving muscovite (Mus), an aluminum silicate mineral ( $Als = Al_2SiO_5$ , andalusite, sillimanite or kyanite), biotite (Bio), cordierite (Cdt) and silicate liquids (Liq) saturated with quartz (Qtz), alkali feldspar (Ksp) and plagioclase (Pl). Building on the work of Thompson (1982), it is shown that the AFM liquidus field for Mus ( $Mus + Liq + Qtz + Ksp + Pl$ ) suppresses the liquidus fields for Als ( $Als + Liq + Qtz + Ksp + Pl$ ) and Cdt ( $Cdt + Liq + Qtz + Ksp + Pl$ ). By analogy it is suggested that for  $H_2O$ -undersaturated liquids, the liquidus field for Mus should also suppress a liquidus field for Gar ( $Gar + Liq + Qtz + Ksp + Pl$ ). It follows that at high pressures, all Qtz-Ksp-Pl-saturated AFM liquids conclude ideal fractional crystallization on the  $Qtz + Ksp + Pl + Mus + Bio = Liq$  reaction. This accounts for the observation that most muscovite-bearing granites also have biotite, but no other AFM minerals. The appearance of garnet late during fractional crystallization is attributable to the non-AFM component MnO. Spessartine-rich garnet crystallizes when the liquid, biotite and muscovite become saturated with  $Mn^{2+}$ .

**Keywords:** AFM projection, granite system, liquidus reactions, muscovite-bearing granites, Mn-rich garnet.

### SOMMAIRE

La projection AFM ( $A = Al_2O_3 - K_2O - Na_2O - CaO$ ,  $F = FeO$ ,  $M = MgO$ ) est idéale pour illustrer les réactions de liquidus qui impliquent la muscovite (Mus), un silicate d'aluminium naturel ( $Als = Al_2SiO_5$ , andalousite, sillimanite ou disthène), la biotite (Bio), la cordiérite (Cdt) et des liquides silicatés (Liq) saturés en quartz (Qtz), feldspath alcalin (Ksp) et plagioclase (Pl). Suite au travail de Thompson (1982), on montre que le champ du liquidus AFM pour Mus ( $Mus + Liq + Qtz + Ksp + Pl$ ) supprime les champs de liquidus pour Als ( $Als + Liq + Qtz + Ksp + Pl$ ) et Cdt ( $Cdt + Liq + Qtz + Ksp + Pl$ ). Par analogie on propose que, pour les liquides sous-saturés en  $H_2O$ , le champ de liquidus pour Mus devrait également supprimer un champ de liquidus pour Gar ( $Gar + Liq + Qtz + Ksp + Pl$ ). Il s'ensuit qu'à haute pression tous les liquides saturés en Qtz-Ksp-Pl terminent une cristallisation fractionnée idéale par la réaction  $Qtz + Ksp + Pl + Mus + Bio = Liq$ . Voilà qui explique l'observation que la plupart des granites à muscovite tiennent aussi de la biotite, quoique sans aucun autre minéral AFM. L'apparition tardive du grenat au cours de la cristallisation fractionnée peut être attribuée à un composant non-AFM, à savoir MnO. Un grenat riche en spessartine

cristallise lorsque liquide, biotite et muscovite atteignent la saturation en  $Mn^{2+}$ .

(Traduit par la Rédaction)

**Mots-clés:** projection AFM, système granitique, réactions de liquidus, granites à muscovite, grenat riche en Mn.

### INTRODUCTION

The partial melting of pelitic rocks during prograde metamorphism is believed to be responsible for some S-type (Chappell & White 1974) granitic magmas. In what is probably the most acceptable scenario, a hydrous vapor phase is absent, or the activity of  $H_2O$ ,  $a(H_2O) = P(H_2O)/P(\text{total})$ , is less than one (Lundgren 1966, Fyfe 1969, Grant 1973, Harris 1974, Thompson & Algor 1977, Thompson & Tracy 1979, Clemens & Wall 1981, Thompson 1982, Clemens 1984). Melting commences in response to the  $H_2O$  released by the breakdown of an important hydrous mineral, such as muscovite, at a higher temperature than that for the P-T locus of the  $H_2O$ -saturated liquidus minimum in the system  $NaAlSi_3O_8 - KAlSi_3O_8 - SiO_2 - H_2O$ , i.e., the haplogranite liquidus minimum of Tuttle & Bowen (1958).

The chemistry of the initial silicate liquid is dominated by the haplogranite components,  $NaAlSi_3O_8 - KAlSi_3O_8 - SiO_2 - H_2O$ , especially for liquids saturated with respect to quartz, two feldspars and a vapor phase (Abbott & Clarke 1979, Thompson 1982, Clemens 1984). Such multiply-saturated liquids will dissolve only minor amounts of other components like FeO, MgO or normative  $Al_2O_3$ . Consequently, the influence of these 'other' components on the liquidus equilibria involving the haplogranite minerals (quartz and the feldspars) is commensurately small. FeO, MgO and normative  $Al_2O_3$  have the effect of displacing to a lower temperature the liquidus minimum saturated in quartz, two feldspars and  $H_2O$ , but not by more than approximately  $20^\circ C$  (Abbott & Clarke 1979, Thompson 1982).

For liquids saturated with respect to quartz, two feldspars and a vapor phase, the liquidus reactions can be represented conveniently in Thompson's (1957) AFM projection ( $A = Al_2O_3 - K_2O - Na_2O - CaO$ ,  $F = FeO$ ,  $M = MgO$ ) (Abbott &

Clarke 1979, Abbott 1981). The liquidus surface saturated in quartz, two feldspars and vapor in the AFM projection is comparatively flat. For any given  $P(\text{total})$  and  $a(\text{H}_2\text{O})$ , it is doubtful that the relief on the surface (in terms of temperature) could ever be more than approximately  $20^\circ\text{C}$  (Abbott & Clarke 1979, Thompson 1982). The relevant AFM liquidus reactions for low pressures, where muscovite is not possible, have been derived by Abbott & Clarke (1979). For high pressures, where muscovite is possible, the end-member AF and AM liquidus reactions have been carefully determined by Thompson (1982).

The purpose of this exercise is to determine the ternary AFM liquidus relationships involving muscovite in order to extend both my own work (Abbott & Clarke 1979, Abbott 1981) and that of Thompson (1982). The essential ingredients for this work can be found in Thompson (1982).

#### BASIS FOR DETERMINING AFM LIQUIDUS REACTIONS

According to the Alkemade rule (Ehlers 1972), for every liquidus equilibrium  $\text{Liq} + \text{A} + \text{B} + \text{C} + \dots + \text{N}$ , where A, B, C, ... and N are minerals, there is a corresponding subsolidus equilibrium  $\text{A} + \text{B} + \text{C} + \dots + \text{N}$ . The form of the reaction, whether it is even ( $\text{A} + \text{B} + \text{C} + \dots + \text{N} = \text{Liq}$ ) or odd (e.g.,  $\text{B} + \text{C} + \dots + \text{N} = \text{A} + \text{Liq}$ ) using the terminology of Ricci (1951), is uniquely determined by the shape of the liquidus. The shape of the liquidus, hence the form of the liquidus reaction, is controlled by the locus of the liquid composition relative to the region of compositional space defined by the coexisting solidus minerals  $\text{A} + \text{B} + \text{C} + \dots + \text{N}$ . For an N-dimensional compositional region (N minerals), there is only one possible even reaction, whereas the number of possible odd reactions is

$$\left[ \sum_{n=0}^N \frac{N!}{n!(N-n)!} \right] - 2$$

It does not follow that for each 'immediately' subsolidus equilibrium  $\text{A} + \text{B} + \text{C} + \dots + \text{N}$  there is a uniquely defined liquidus reaction, because the shape of the liquidus cannot be determined on the basis of the subsolidus equilibria alone. It is, however, true that for each "immediately" subsolidus equilibrium  $\text{A} + \text{B} + \text{C} + \dots + \text{N}$  there is a corresponding liquidus equilibrium  $\text{Liq} + \text{A} + \text{B} + \text{C} + \dots + \text{N}$ . But the form of the liquidus reaction, whether it is even or one of the odd possibilities, cannot be specified without knowing the composition of the liquid and the composition of the coexisting minerals.

In the context of the AFM projection, the various 2- and 3-phase subsolidus equilibria may be treated as Alkemade lines and triangles, respectively (Abbott & Clarke 1979, Abbott 1981). For each Alkemade line connecting two subsolidus minerals  $\text{A} + \text{B}$ , there is an AFM liquidus equilibrium  $\text{A} + \text{B} + \text{Liq}$ , which is represented on the liquidus surface by the locus of liquids coexisting with  $\text{A} + \text{B}$ . The form of the reaction,  $\text{A} + \text{B} = \text{Liq}$  (even),  $\text{A} = \text{B} + \text{Liq}$  (odd), or  $\text{B} = \text{A} + \text{Liq}$  (odd), is ambiguous. For each Alkemade triangle relating three subsolidus phases  $\text{A} + \text{B} + \text{C}$ , there is an AFM liquidus equilibrium  $\text{A} + \text{B} + \text{C} + \text{Liq}$ , which is represented on the liquidus surface by the composition of the liquid coexisting with  $\text{A} + \text{B} + \text{C}$ . Again, the form of the reaction, one even possibility ( $\text{A} + \text{B} + \text{C} = \text{Liq}$ ) and six odd possibilities, is ambiguous. Even though the odd-even character of each equilibrium cannot be determined simply on the basis of the Alkemade lines and triangles (subsolidus equilibria), the connectivity of the liquidus equilibria is uniquely determined.

The odd-even ambiguity can be circumvented if the following assumptions are adopted (Abbott & Clarke 1979, Abbott 1981): 1) On the AFM liquidus surface, for any given  $P(\text{total})$  and  $a(\text{H}_2\text{O})$ , there is only one minimum to which all ternary AFM liquids proceed during ideal fractional crystallization. 2) The ratio of  $\text{FeO}/(\text{MgO} + \text{FeO})$  in the liquid is higher than in the coexisting AFM mineral assemblage. If so, it follows that the liquidus minimum is on the AF join (Thompson 1982). This is supported by experimental results reported by Hensen & Green (1971). However, Green (1976) and Clemens & Wall (1981) reported the results of experiments suggesting that the ratio of  $\text{FeO}/(\text{MgO} + \text{FeO})$  is higher in garnet than in the coexisting liquid. The conclusion of Clemens & Wall (1981) is based on almandine-seeded charges. The initial value of the ratio  $\text{FeO}/(\text{MgO} + \text{FeO})$  was higher in the garnet than the glass. There is no demonstration that the composition of the garnet achieved equilibrium with the coexisting liquid. In the earlier experiments by Green

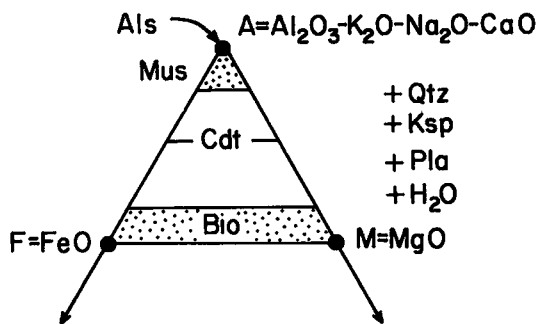


FIG. 1. AFM projection from quartz (Qtz), alkali feldspar (Ksp), plagioclase (Pl) and  $\text{H}_2\text{O}$  (Thompson 1957), showing the range of composition for muscovite (Mus), biotite (Bio), cordierite (Cdt) and an aluminum silicate mineral (Als = andalusite, kyanite or sillimanite).  $\text{A} = \text{Al}_2\text{O}_3\text{-K}_2\text{O-Na}_2\text{O-CaO}$ ,  $\text{M} = \text{MgO}$ ,  $\text{F} = \text{FeO}$ .

(1976), substantial iron loss to the platinum capsules was acknowledged. Also, disequilibrium is suggested in the form of crossing tie-lines involving the ratio of  $\text{FeO}/(\text{MgO} + \text{FeO})$  in garnet and the coexisting liquid.

For the purposes of this paper the only AFM minerals that need to be considered are an aluminum silicate ( $\text{Als} = \text{Al}_2\text{SiO}_5$ , andalusite, sillimanite or kyanite), biotite (Bio), cordierite (Cdt), muscovite (Mus) and garnet (Gar). For granitic rocks, the partitioning of Fe and Mg in terms of  $X_{\text{Fe}} = \text{FeO}/(\text{MgO} + \text{FeO})$  is  $X_{\text{Fe}}(\text{Mus}) > X_{\text{Fe}}(\text{Bio})$  [inferred from reaction 5 of Thompson (1982)],  $X_{\text{Fe}}(\text{Gar}) > X_{\text{Fe}}(\text{Bio})$  and  $X_{\text{Fe}}(\text{Bio}) > X_{\text{Fe}}(\text{Cdt})$  (Thompson 1982, Clarke 1981). The projected ranges of composition for the different minerals are shown in Figure 1. The claudonite components  $\text{KMgAlSi}_4\text{O}_{10}(\text{OH})_2$  and  $\text{KFeAlSi}_4\text{O}_{10}(\text{OH})_2$  account for ternary muscovite (Miller *et al.* 1981).

Figure 2 illustrates schematically the various AF, AM and AFM subsolidus and liquidus reactions. The reactions are written in terms of the AFM phases only. Quartz, alkali feldspar, plagioclase and  $\text{H}_2\text{O}$  are involved as needed to balance each reaction. The reactions shown as fine lines are from Thompson (1982) and numbered according to his scheme. The four reactions in bold lines identified by the letters A, B, C and D are introduced here. Reactions 5', 24, 33', 34', 36', 39' and 42' are on the AF join. Reactions 4'', 23'', 33'', 36'', 39'', 42'' and 71'' are on the AM join. Reactions 64', A, B, C, and D are ternary AFM reactions. Reactions 2', 28' and E take place at A, in the AFM projection.

The reactions 24, 5', A, 4'', 2' and 23'' divide the subsolidus P-T space into 7 regions, respectively characterized by 7 AFM topologies,  $S_1$  through  $S_7$ . Each of the six subsolidus reactions terminates at one of the invariant points  $I_1$  through  $I_6$ , each of which involves a liquid.  $I_5$  is equivalent to Thompson's (1982)  $I_3$ . The ternary invariant point  $I_3$  is introduced in this study. The arrangement of the stable and metastable parts of the reactions around each invariant point was determined by a Schreinemaker analysis. The six invariant points define seven ranges of pressure, for each of which there is a corresponding AFM liquidus topology,  $L_1$  through  $L_7$ . The binary AF and AM liquidus reactions are from Thompson (1982). The ternary AFM liquidus reactions and topologies  $L_1$  through  $L_7$  were predicted on the basis of the corresponding subsolidus AFM topologies  $S_1$  through  $S_7$  and the assumptions outlined earlier in this section.

Because all of the liquids in Figure 2 are saturated with respect to quartz, two feldspars and  $\text{H}_2\text{O}$  vapor, for any given pressure, all liquidus reactions in Figure 2 occur within a very narrow range of temperature, not more than approximately 20°C below the liquidus minimum in the haplogranite system

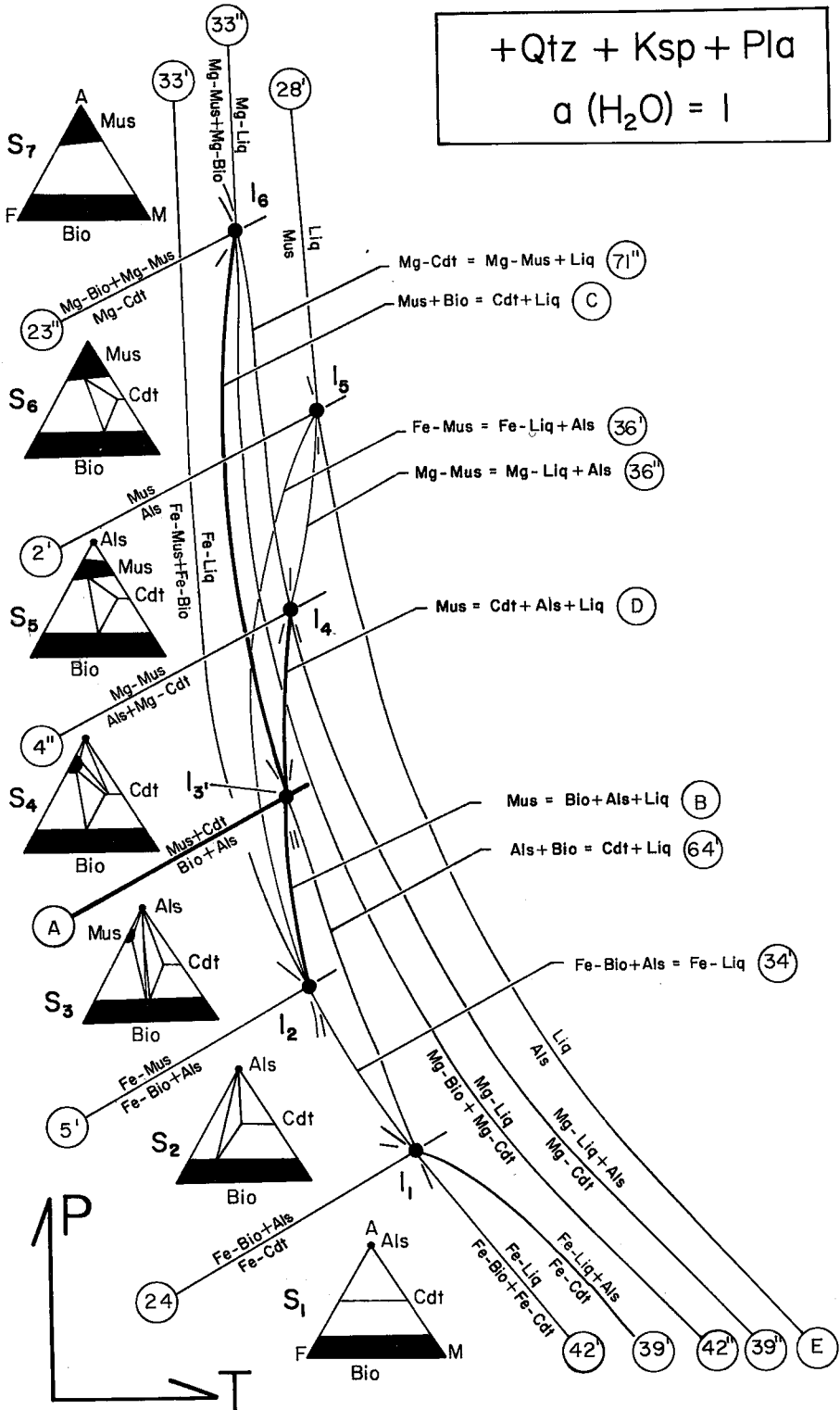
$\text{KAlSi}_3\text{O}_8\text{-NaAlSi}_3\text{O}_8\text{-SiO}_2\text{-H}_2\text{O}$  (Abbott & Clarke 1979, Thompson 1982).

Thompson (1982) showed that for the Na-Ca-free AFM system, at any given pressure, reactions 5, A, 4, 2 and 23 may all occur within a range of temperature less than 10°C. Consequently, the difference in pressure between AF invariant point  $I_2$  and AM invariant point  $I_6$  may be less than 0.5 kilobar (Fig. 5, Thompson 1982). The invariant points  $I_3$ ,  $I_4$  and  $I_5$  ( $= I_3$  of Thompson 1982) necessarily occur in the narrow range of pressure between  $I_2$  and  $I_6$ . The relationships for the Na-Ca-free system are shown in Figure 3, adapted from Thompson (1982, Fig. 5).

The AFM liquidus topologies  $L_3$ ,  $L_4$ ,  $L_5$  and  $L_6$  are restricted to such a narrow range of pressure that for practical purposes, they cannot be shown in Figure 3. With increasing pressure, the AFM liquidus field for muscovite expands and effectively eliminates the liquidus fields for Als and Cdt within a pressure interval as small as 0.5 kilobar (Thompson 1982). It can be inferred that for liquids saturated in quartz-two feldspars-vapor, primary muscovite coexisting with Als, Cdt or both should be exceedingly rare (Table 1). At high pressures, where primary muscovite is possible, two-mica granites (topology  $L_7$ ) should be relatively common (Table I). A compilation by Armstrong & Boudette (1984) of about 300 modal compositions of two-mica granites, from a much smaller number of plutons, suggests that most muscovite-biotite granites do not contain other AFM minerals. Clarke (1981) showed 76 muscovite-bearing AFM mineral assemblages from a much smaller number of granitic plutons. Only 10 (13%) of Clarke's (1981) assemblages have, in addition to muscovite  $\pm$  biotite, other AFM minerals (Gar, Cdt or Als).

#### REDUCED $a(\text{H}_2\text{O})$

As the activity of  $\text{H}_2\text{O}$ ,  $a(\text{H}_2\text{O})$ , decreases, the subsolidus reactions are displaced to lower temperatures and the liquidus equilibria are displaced to higher temperatures (Thompson & Algor 1977, Kerrick 1972, Holdaway & Lee 1977, Abbott & Clarke 1979) such that each of the invariant points  $I_1$  through  $I_6$  is translated to higher pressures and higher temperatures. Thompson's (1982) reaction 30' is the locus of  $I_5$  (Fig. 4) for  $a(\text{H}_2\text{O}) < 1$ . The locus of  $I_1$  has been described by Abbott & Clarke (1979). The loci of  $I_2$ ,  $I_3$ ,  $I_4$  and  $I_6$  are parallel and very close to the locus of  $I_5$  (reaction 30'). The loci define several P-T regions, each characterized by a distinct  $\text{H}_2\text{O}$ -undersaturated AFM liquidus topology saturated in quartz and the two feldspars (Fig. 4). The high-temperature - low-pressure liquidus topologies (not involving muscovite) are from Abbott & Clarke (1979). It is proposed here that the AFM liquidus field for muscovite eliminates the liquidus



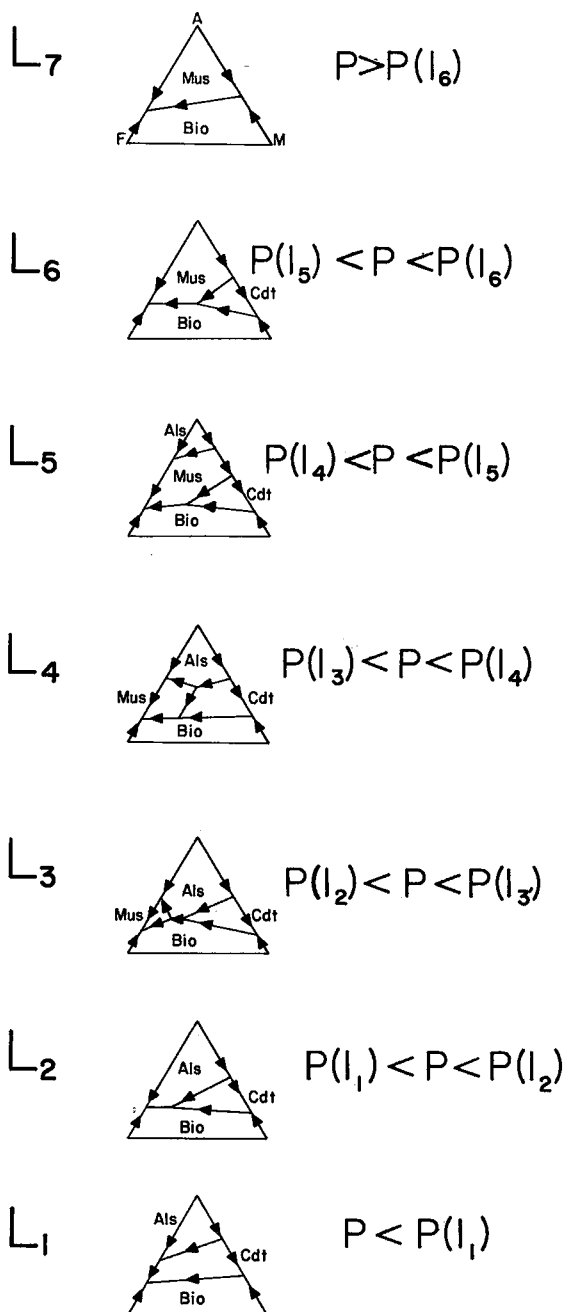


FIG. 2. Schematic subsolidus and liquidus reactions in which all liquids are saturated with respect to Qtz, Ksp, Pla and H<sub>2</sub>O. The subsolidus reactions 24, 5', 4", 2', 23" and liquidus reactions 28', 33", 33', 34', 36', 36", 39', 39", 42', 42", 64' and 71" are from Thompson (1982). The remaining reactions, shown as bold lines, are introduced here. There are 6 invariant points, I<sub>1</sub> through I<sub>6</sub>, which define 7 pressure regimes, each of which is characterized by one of the AFM liquidus diagrams L<sub>1</sub> through L<sub>7</sub>.

# System, $K_2O$ - $MgO$ - $FeO$ - $Al_2O_3$ - $SiO_2$ - $H_2O$ a ( $H_2O$ ) = 1

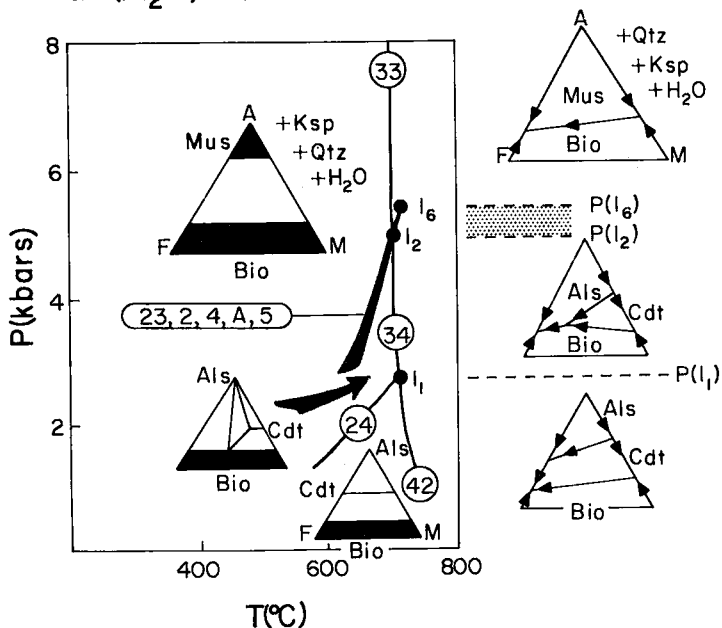


FIG. 3. Semiquantitative P-T diagram based on Thompson (1982, Fig. 5) showing selected reactions in the system  $K_2O$ - $MgO$ - $FeO$ - $Al_2O_3$ - $SiO_2$ - $H_2O$ . The reactions correspond by number to those illustrated schematically in Figure 2 for the full system  $K_2O$ - $Na_2O$ - $CaO$ - $MgO$ - $FeO$ - $Al_2O_3$ - $SiO_2$ - $H_2O$ . All liquids are saturated with respect to Qtz, Ksp and  $H_2O$ . There are three important AFM ( $A = Al_2O_3$ - $K_2O$ ) liquidus topologies,  $L_1$ ,  $L_2$ , and  $L_7$  (see Fig. 2).

field for garnet [where  $a(H_2O) < 1$ ] just as effectively as it eliminates the liquidus fields for cordierite and aluminum silicate (Als).

TABLE 1. STATISTICS ON MUSCOVITE-BEARING GRANITES, QUARTZ MONZONITES AND GRANDIODORITES, BASED ON MODAL ANALYSES FROM JOHANNSEN'S (1932) INTRUSIVE ROCK FAMILIES 226<sup>P</sup>, 226<sup>Q</sup>, 227<sup>P</sup> and 227<sup>Q</sup>

Number of analyses	200	Percentage of muscovite-bearing modal analyses
Number of modal analyses with muscovite	30	3.3%
Number of modal analyses with muscovite, but no other AFM minerals	1	3.3%
Number of modal analyses with muscovite + biotite, but no other AFM minerals	22	73.3%
Number of modal analyses with muscovite + biotite + hornblende, but no other AFM minerals	5	16.7%
Number of modal analyses with muscovite + biotite + garnet, but no other AFM minerals	2	6.7%
Number of modal analyses with muscovite + garnet, but no other AFM minerals	0	0%

## DISCUSSION

Many granites show evidence consistent with the saturation of the liquid with respect to quartz and two feldspars throughout the crystallization history. Similarly, many restite assemblages in migmatites have quartz and two feldspars (Clemens 1984), indicating that the liquid was saturated with respect to these minerals throughout the melt-producing event. For such granites and migmatites, the AFM liquidus topologies shown in Figure 4 are particularly relevant. The liquidus topologies can be used, like liquidus diagrams for conventional ternary systems, to predict changes in the AFM mineral assemblages during melting or during crystallization. Conversely, the mineral assemblage and textural relationships in a migmatite or granite may prove to be compatible with only one of the AFM liquidus topologies. If so, Figure 4 can be used like a petrogenetic grid to help characterize P, T and  $a(H_2O)$ . Examples are given in Abbott & Clarke (1979), Abbott (1981) and Speer (1981).

It should be noted that the AFM liquidus topo-

gies in Figures 2, 3 and 4 are only applicable to systems saturated with respect to quartz and two feldspars. Muscovite schist containing quartz and plagioclase but no alkali feldspar must be referred to a different set of equilibria. This would be a severe limitation with regard to the anatexis of pelitic mineral assemblages, except that the assemblage muscovite + quartz + plagioclase melts incongruently to alkali feldspar, Al<sub>2</sub>SiO<sub>5</sub> and liquid along reaction 30' (Fig. 4) where  $a(\text{H}_2\text{O}) < 1$ . In this reaction, the H<sub>2</sub>O released by the breakdown of the muscovite is partitioned into the liquid, which is then saturated with respect to quartz, plagioclase and alkali feldspar, but undersaturated with respect to H<sub>2</sub>O. If the liquid is removed from the restite,  $a(\text{H}_2\text{O})$  would increase in the liquid during fractional crystallization according to the AFM liquidus diagram appropriate for the pressure and  $a(\text{H}_2\text{O})$ . For high pressures, in the context of Figures 3 and 4, it is difficult to conceive of a situation in which ideal fractional crystallization is not concluded on the AFM equilibrium Bio + Mus + Liq. Thus, it is not surprising that approximately 73% of all muscovite-bearing granites have biotite, but no other AFM minerals (Table 1).

The relationships shown in Figure 4 suggest that garnet-muscovite granites and garnet-biotite-muscovite granites should not exist. Yet, these assemblages are relatively common in late pegmatites and aplite dykes (Miller & Stoddard 1978, 1981, Deer *et al.* 1982). The appearance of garnet late in the fractional crystallization of muscovite-saturated granitic magmas is probably due to the partitioning of manganese into the liquid rather than into early minerals. The garnet in pegmatites, aplite dykes and granites is characteristically high in spessartine (Miller & Stoddard 1978, 1981, Deer *et al.* 1982, Clarke 1981). This, combined with an apparent intolerance of biotite for high Mn<sup>2+</sup>, suggests (Hall 1965, Miller & Stoddard 1978, 1981, Abbott 1981) that garnet crystallizes when the melt, the muscovite and the biotite become saturated with respect to Mn<sup>2+</sup>. Figure 5 illustrates the presumed effect of increasing the molar ratio MnO/(FeO + MgO + MnO).

### CONCLUSIONS

1. For liquids saturated with respect to quartz, two feldspars and H<sub>2</sub>O, the reactions can be conveniently represented in an AFM liquidus diagram (Abbott & Clarke 1979, Abbott 1981).
2. The details of the appearance or disappearance of a liquidus field for muscovite are complicated (Fig. 2).
3. There is one important AFM liquidus topology (L<sub>7</sub>) involving muscovite, because the liquidus field for muscovite suppresses the AFM liquidus equilibria Liq + Cdt, Liq + Als, and Liq + Gar. This happens

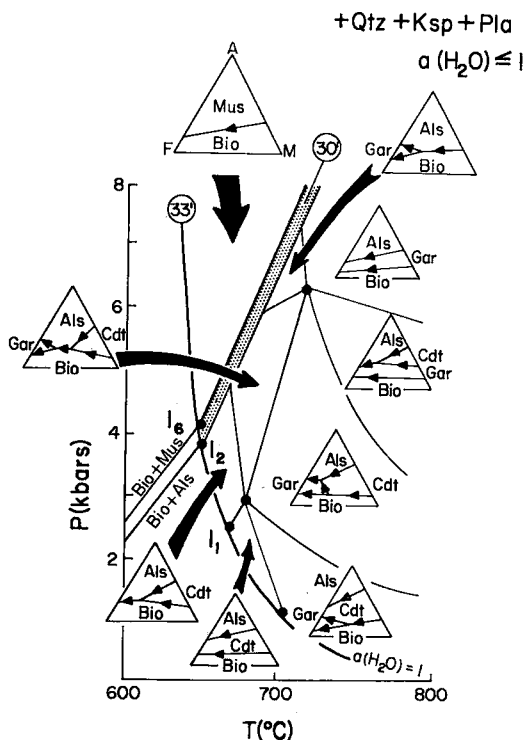


FIG. 4. Regions of distinct AFM liquidus topologies in P-T space as a function of  $a(\text{H}_2\text{O}) \leq 1$ . All liquids are saturated with respect to Qtz, Ksp and Pla. The locus of liquidus minima for  $a(\text{H}_2\text{O}) = 1$  is based on Tuttle & Bowen (1958). The loci of invariant points  $I_2$ ,  $I_3$ ,  $I_4$ ,  $I_5$  and  $I_6$  lie in the stippled band. The locus of  $I_5$  is Thompson's (1982) reaction 30', Pla + Qtz + Mus = Ksp + Als + Liq. Between the locus of H<sub>2</sub>O-saturated minima and the stippled band there is one AFM liquidus topology for liquids saturated with respect to Qtz, Pla and Ksp. The liquidus field for Mus effectively suppresses the equilibria Liq + Gar, Liq + Cdt and Liq + Als. The H<sub>2</sub>O-undersaturated AFM liquidus topologies for high temperatures and low pressures (not involving Mus) are from Abbott & Clarke (1979).

even for reduced  $a(\text{H}_2\text{O})$  as long as there is a liquidus field for muscovite (Fig. 4).

4. For all AFM liquids at high pressure, ideal fractional crystallization is concluded on the AFM reaction Bio + Mus = Liq. This accounts for the observation that most muscovite-bearing granites also contain biotite but are devoid of other AFM minerals (Table 1).

5. The appearance of garnet late during fractional crystallization is attributable to strong partitioning of Mn<sup>2+</sup> into the liquid relative to muscovite or biotite (Fig. 5).

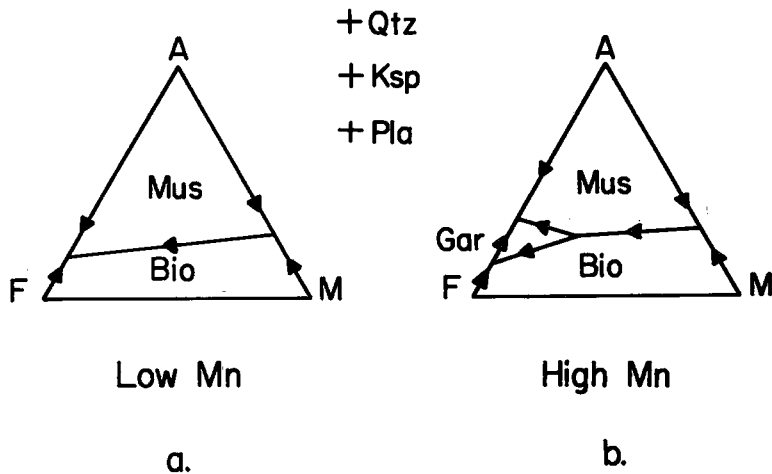


FIG. 5. Suggested changes in the liquidus topology  $L_7$  in response to a high concentration of  $Mn^{2+}$ . a. AFM liquidus topology  $L_7$  where the ratio of  $MnO/(FeO + MgO + MnO)$  is low. b. The appearance of the liquidus field for garnet where  $MnO/(FeO + MgO + MnO)$  is high.

#### ACKNOWLEDGEMENTS

I thank the following individuals for their helpful comments: D.B. Clarke, J.D. Clemens, R.F. Martin, C.F. Miller and J.A. Speer.

#### REFERENCES

- ABBOTT, R.N., JR. (1981): AFM liquidus projections for granitic magmas, with special reference to hornblende, biotite and garnet. *Can. Mineral.* **19**, 103-110.
- \_\_\_\_\_ & CLARKE, D.B. (1979): Hypothetical liquidus relationships in the subsystem  $Al_2O_3$ -FeO-MgO projected from quartz, alkali feldspar and plagioclase for  $a(H_2O) \leq 1$ . *Can. Mineral.* **17**, 549-560.
- ARMSTRONG, E.L. & BOUDETTE, E.L. (1984): Two mica granites. A. Their occurrence and petrography. *U.S. Geol. Surv., Open File Rep.* **OF84-0173**.
- CHAPPELL, B.W. & WHITE, A.J.R. (1974): Two contrasting granite types. *Pacific Geol.* **8**, 173-174.
- CLARKE, D.B. (1981): The mineralogy of peraluminous granites: a review. *Can. Mineral.* **19**, 3-17.
- CLEMENS, J.D. (1984): Water contents of silicic to intermediate magmas. *Lithos* **17**, 273-287.
- \_\_\_\_\_ & WALL, V.J. (1981): Origin and crystallization of some peraluminous (S-type) granitic magmas. *Can. Mineral.* **19**, 111-131.
- DEER, W.A., HOWIE, R.A. & ZUSSMAN, J. (1982): *Rock-Forming Minerals. 1A. Orthosilicates (2nd edition)*. Longman, London.
- EHLERS, E.G. (1972): *The Interpretation of Geological Phase Diagrams*. W.H. Freeman & Co., San Francisco.
- FYFE, W.S. (1969): Some thoughts on granitic magmas. In *Mechanism of Igneous Intrusion* (G. Newall & N. Rast, eds.). *Geol. J., Spec. Issue 2*, 201-216.
- GRANT, J.A. (1973): Phase equilibria in high-grade metamorphism and partial melting of pelitic rocks. *Amer. J. Sci.* **273**, 289-317.
- GREEN, T.H. (1976): Experimental generation of cordierite- or garnet-bearing granitic liquids from a pelitic composition. *Geology* **4**, 85-88.
- HALL, A. (1965): The origin of accessory garnet in the Donegal granite. *Mineral. Mag.* **36**, 628-633.
- HARRIS, N.B.W. (1974): The petrology and petrogenesis of some muscovite granite sills from the Barousse Massif, central Pyrenees. *Contr. Mineral. Petrology* **45**, 215-230.
- HENSEN, B.J. & GREEN, D.H. (1971): Experimental study of the stability of cordierite and garnet in pelitic compositions at high pressures and temperatures. *Contr. Mineral. Petrology* **33**, 309-330.
- HOLDAWAY, M.J. & LEE, S.M. (1977): Fe-Mg cordierite stability in high-grade pelitic rocks based on experimental, theoretical, and natural observations. *Contr. Mineral. Petrology* **63**, 175-198.

- JOHANNSEN, A. (1932): *A Descriptive Petrography of the Igneous Rocks. II. The Quartz-Bearing Rocks.* University of Chicago Press, Chicago, Ill.
- KERRICK, D.M. (1972): Experimental determination of muscovite + quartz stability with  $P_{H_2O} < P_{total}$ . *Amer. J. Sci.* **272**, 946-958.
- LUNDGREN, L.W., JR. (1966): Muscovite reactions and partial melting in south-eastern Connecticut. *J. Petrology* **7**, 421-453.
- MILLER, C.F. & STODDARD, E.F. (1978): Origin of garnet in granitic rocks: an example of the role of Mn from the Old Woman - Piute Range, California. *Geol. Assoc. Can. - Mineral. Assoc. Can. Abstr. Programs* **3**, 456.
- \_\_\_\_\_ & \_\_\_\_\_ (1981): The role of manganese in the paragenesis of magmatic garnet: an example from the Old Woman - Piute Range, California. *J. Geol.* **89**, 233-246.
- \_\_\_\_\_, \_\_\_\_\_, BRADFISH, L.J. & DOLLASE, W.A. (1981): Composition of plutonic muscovite: genetic implications. *Can. Mineral.* **19**, 25-34.
- RICCI, J.E. (1951): *The Phase Rule and Heterogeneous Equilibrium.* Van Nostrand, New York.
- SPEER, J.A. (1981): Petrology of cordierite- and almandine-bearing granitoid plutons of the southern Appalachian Piedmont, U.S.A. *Can. Mineral.* **19**, 35-46.
- THOMPSON, A.B. (1982): Dehydration melting of pelitic rocks and the generation of H<sub>2</sub>O-undersaturated granitic liquids. *Amer. J. Sci.* **282**, 1567-1595.
- \_\_\_\_\_ & ALGOR, J.R. (1977): Model systems for anatexis of pelitic rocks. I. Theory of melting reactions in the system KAlO<sub>2</sub>-NaAlO<sub>2</sub>-Al<sub>2</sub>O<sub>3</sub>-SiO<sub>2</sub>-H<sub>2</sub>O. *Contr. Mineral. Petrology* **63**, 247-269.
- \_\_\_\_\_ & TRACY, R.J. (1979): Model systems for anatexis of pelitic rocks. II. Facies series melting and reactions in the system CaO-KAlO<sub>2</sub>-NaAlO<sub>2</sub>-Al<sub>2</sub>O<sub>3</sub>-SiO<sub>2</sub>-H<sub>2</sub>O. *Contr. Mineral. Petrology* **70**, 429-438.
- THOMPSON, J.B., JR. (1957): The graphical analysis of mineral assemblages in pelitic schists. *Amer. Mineral.* **42**, 842-858.
- TUTTLE, O.F. & BOWEN, N.L. (1958): The origin of granite in the light of experimental studies in the system NaAlSi<sub>3</sub>O<sub>8</sub>-KAlSi<sub>3</sub>O<sub>8</sub>-SiO<sub>2</sub>-H<sub>2</sub>O. *Geol. Soc. Amer. Mem.* **74**.

Received December 3, 1984, revised manuscript accepted April 22, 1985.